ARTICLE

Electro-active Shape Memory Properties of Poly(ε-caprolactone)/Functionalized Multiwalled Carbon Nanotube Nanocomposite

Yu Xiao, Shaobing Zhou,* Lin Wang, and Tao Gong

School of Materials Science and Engineering, Key Laboratory of Advanced Technologies of Materials, Ministry of Education, Southwest Jiaotong University, Chengdu, 610031, P. R. China

ABSTRACT One type of electroactive shape memory nanocomposite was fabricated, including cross-linked poly(ε-caprolactone) (cPCL) and conductive multiwalled carbon nanotubes (MWNTs). The cross-linking reaction of the pristine poly(ε-caprolactone) (PCL) was realized by using benzoyl peroxide (BPO) as an initiator. The raw MWNTs (Raw-M) were prefunctionalized by acid-oxidation process and covalent grafting with poly (ethylene glycol) (PEG), respectively. Three kinds of nanocomposites containing cPCL/Raw-M, cPCL/acid-oxidation MWNTs (AO-M) and cPCL/PEG grafted MWNTs (PEG-M) were obtained, and the mechanical, electrical and shape memory properties were further investigated. The influence of in vitro degradation on their shape memory and mechanical properties was also evaluated. The methyl thiazolyl tetrazolium (MTT) assay was performed to estimate their biocompatibility. The results displayed that these nanocomposites could perform favorable shape memory recovery both in hot water at 55 °C and in electric field with 50 V applied voltage. In addition, compared with cPCL/Raw-M and cPCL/AO-M, cPCL/PEG-M composite possessed more favorable properties such as mechanical, biocompatible, and electroactive shape memory functions. Therefore, the nanocomposite may be potential for application as smart bioactuators in biomedical field.

KEYWORDS: shape memory • carbon nanotube • biodegradable • nanocomposites

INTRODUCTION

Shape memory polymers (SMPs), as a family of smart materials that can be deformed into temporary shape and soon recover their original shape under a certain external stimulus, have been drawing more and more attention because of their novel properties (1−4). However, there still exist some problems such as poor mechanical property that largely restrict the SMPs to achieve their scientific and technological significance in biomedical field (5, 6). Moreover, conventionally, the deformation and recovery process of SMPs are usually induced by direct thermal stimulus, and the temperature with this triggering method must be above the transition temperature of SMPs such as melting temperature or glass transition temperature (7, 8). However, the temperature is always far from the normal body's temperature and sometimes even does harm to human body. Therefore, a key challenge is that a safer and more effective stimulus is necessary when SMPs are used as in vivo medical devices (9, 10).

Nowadays, some other stimulus method such as electric field (11, 12), magnetic field (13−15), water/solvent (16, 17), and light (18, 19) are discovered by many researchers. Among those triggering stimuli, electric-field stimulation plays a more and more important role in view of its convenient manipulation, high reliability, and wide application (9). To date, some researchers have prepared various kinds of electro-active SMPs. These SMPs are always filled with electrical conductive fillers such as carbon nanotubes, carbon particles, carbon fibers, nickel zinc ferrite ferromagnetic particles, etc. (20−31). For example, an electroactive shape-memory polyurethane with 5 wt % multiwalled carbon nanotubes (MWNTs) was synthesized by Cho and his co-workers, and they proved that the shape of these SMPs can easily recover under 40 V supplied voltage within 10 s (25). Although a lot of similar research has been performed, few researchers have paid attention to the biocompatibility of these electroactive SMPs, the biodegradability, and smart function. In fact, these properties are quite vital if SMPs are to be considered as temporary implant materials.

A series of nanocomposites composed of polylactide (PLA) and hydroxyapatite (HA) were successfully synthesized in our group, which have a perfect combination with shape memory properties and biodegradability (5, 32). The cross-linked poly(ε-caprolactone) (cPCL)/Fe_3O_4 nanocomposites were also fabricated and they possess not only fantastic magnetism sensitivity shape memory properties but also good biocompatibility and biodegradability (13, 33).

In this study, we will demonstrate a new kind of electro-active SMPs composed of conductive multiwalled carbon nanotubes (MWNTs) as filler and cPCL as polymer matrix. As we know, MWNTs are arousing more and more interests because of their exceptional combination of mechanical, electrical, thermal, chemical, and optical properties (34, 35). Here, MWNTs were also selected as inductive heat source to stimulate the shape recovery of cPCL matrix. However, there are still some drawbacks for MWNTs such as high toxicity and hydrophobicity, which limit their wide applica-

* Corresponding author. Tel: 86-28-87634023. Fax: 86-28-87634649. E-mail: shaobingzhou@swjtu.cn; shaobingzhou@hotmail.com.
Received for review August 4, 2010 and accepted November 3, 2010

DOI: 10.1021/am100692n

Published on Web 11/19/2010

tion in biomedical field. For example, Porter's report related MWNTs' internalization into living cells indicated that carbon nanotubes can be toxic (36). Currently, MWNTs must be functionalized or modified to improve the hydrophilicity and biocompatibility before their use in biomedical field.

Herein, raw MWNTs (Raw-M) were first prefunctionalized through acid-oxidation process and covalent grafting with poly(ethylene glycol) (PEG). Thus, three kinds of MWNTs including Raw-M, acid-oxidation MWNTs (AO-M) and PEG grafted MWNTs (PEG-M) could be obtained. Later, the nanocomposites composed of cPCL and these MWNTs were fabricated. After that, a series of tests were carried out to characterize these nanocomposites' properties including mechanical properties, electrical conductivity, in vitro degradation and cytotoxicity evaluation. Significantly, their shape memory effects were investigated in electric field with 50 V applied voltage and in hot water at 55 °C, respectively, and the shape memory recovery ratio and speed under the two stimuli were further compared (37, 38).

EXPERIMENTAL SECTION

Materials. Linear PCL was synthesized as our previous report (39). The molecular weight (M_w) determined by gel permeation chromatograph (GPC) is 121 000 Da. Benzoyl peroxide (BPO) and poly (ethylene glycol) (PEG, $M_w = 2000$ Da) were purchased from Chengdu Kelong Chemical Reagent Company (Sichuan, Chengdu, China). MWNTs (>95+% purity) with 10−20 nm outer diameters and 10−20 um lengths were purchased from Chengdu Organic Chemistry Limited Company (Sichuan, Chengdu, China). All other chemicals and solvents were of reagent grade or better. The cells which were used in the methyl thiazolyl tetrazolium (MTT) assay were got from the neonatal rat's mandibular osteoblasts.

Fabrication of cPCL and cPCL/MWNT Nanocomposites. Preweighed linear PCL with 3 wt % of BPO was first dissolved in methylene chloride (CH_2Cl_2) under stirring. Then, the solution was cast on a mold, and the solvent was evaporated in aerator overnight and dried at 30 °C under vacuum. Later, the completely dried PCL was kept in an oven at 130 °C for 10 min (because BPO enables cross-linked reaction to occur at 130 °C (40).) As a result, the required slices made up of cPCL with thickness of about 2 mm were obtained.

The prefunctionalized process of raw-M was similar as previous report (41). Briefly, preweighed raw-M were initially added into 70 mL HCl (36.5 wt %) companying with slightly stirring for 2 h, then diluted in water, filtered, washed with deionized water and dried in vacuum at 40 °C overnight. After that, the pretreated MWNTs were put into 50 mL of HNO_3 (65 wt %) under 140 °C heating for 4 h, and then cooled to the room temperature and followed by repeating clean procedures mentioned above. Thus, the acid-oxidation MWNTs (AO-M) were achieved.

PEG-grafted MWNTs (PEG-M) were obtained by a simple esterification method. First, AO-M were put into the CH_2Cl_2 solvent companying with slightly stirring. Then, preweighed *N*,*N*-dicyclohexylcarbodiimide (DCC) and 4-dimethylaminopyridine (DMAP) were added to the AO-M suspension in order to accelerate the reaction speed and restrict the forming of side reaction. The specific process of this reaction can be found in previous report (42).

According to the method reported by Ma et al. (43), each kind of MWNT mentioned above was first dispersed in water with the aid of sodium lauryl sulfate (SLS) under stirring for 30 min in this study. Subsequently, the MWNTs aqueous solution was centrifuged at 20 000 rpm for 10 min to deposit the MWNTs and the MWNTs were dried overnight under vacuum at 40 °C. After that, the mixed solution containing the pretreated MWNTs, pristine PCL and BPO in 20 mL CH_2Cl_2 solvent was achieved companying with the high-energy sonication for 2 h. The followed procedures were similar with the preparation of cPCL as mentioned above. Thus, the cPCL/MWNTs composites were obtained.

Characterization. The surface morphology of MWNTs and polymeric phase in the composites were observed using a Quanta200 Scanning Electron Microscope (SEM, FEI, America). The accelerating voltage was 20 kV.

Static tensile test was accomplished at the crosshead speed of 5 mm/min at room temperature using a universal testing machine Instron 5567 (Instron Co., Massachusetts). Prior to the test the specimens should be cut to dumbbell shape. Of all the mechanical properties, elasticity modulus E, tensile strength δ_b and elongation at break L were tested. Each measurement was repeated 5 times and an average value reported.

Dynamic mechanical analysis (DMA) was carried out on a DMA983 analyzer (Du Pont, America), using a tensile resonant mode at a heating rate of 3 °C/min from 25 to 80 °C and at a frequency of 1 Hz. The storage modulus E' for specimen size 50 × 10 × 2 mm (length × width × thickness) was tested.

Gel fraction estimate was performed by the following method: all the preweighted specimens,m_0, are subjected to swell in CH_2Cl_2 in an attempt to gather gel, which needs 24 h to ensure steady gel fraction values, and then a high speed (15 000 r/min) centrifuge was employed to detach gel from sol. During the process, an observable phenomenon may be noted that some agglomerate of gel floats on the surface of transparent gel solution in the centrifuge tube. Afterward a dried gel mass, m_1, is noted, and the gel fraction can be calculated as follows

$$\text{Gel fraction}\,(\%) = m_1/m_0 \times 100\,\%.$$

A digital four-point probe machine (SZ-82, Hangzhou, China) was employed to evaluate the electrical conductivity of the composites. The electroactive shape memory effect was observed with a kind of self-made equipment which can apply constant voltages to samples. A noncontact thermometer (STPro Manual, Raytek. Co Ltd., China) was used to monitor the temperature change of the samples.

In vitro Degradation. In vitro degradation of all samples was carried out as follows. Preweighed samples were placed individually in test tubes containing 10 mL of 0.1 M phosphate buffered saline (PBS) at pH 7.4. The tubes were kept in a thermostated incubator (Haerbin Dongming Medical Equipment Company) which was maintained at 37 °C and 107 cycles per minute. The degradation process was evaluated from these changes of the molecular weight, gel fraction, shape memory properties and mechanical properties of polymer matrix at predetermined intervals.

Methyl Thiazolyl Tetrazolium (MTT) Assay. The cytotoxicity of all the samples was further evaluated based on the methyl thiazolyl tetrazolium (MTT) assay. The osteoblasts were grown in RPMI medium 1640 (Gibcos) with 10% fetal bovine serum (FBS). The cells with a density of 1.0×10^4 cells/well were cultured in 24 well plates in the above medium and maintained at 37 °C in a humidified incubator with 5% CO_2 and 95% air. After culturing for 1 day, each well was added 0.5 mL MTT (the concentration of MTT is 1 mg/mL). After that the cultures were incubated for 4 h at 37 °C and the supernatants were removed from the wells. Then, 0.5 mL per well of dimethylsulfoxide (DMSO) was added in isopropanol and mixed with the content of the wells thoroughly, and 0.2 mL mixed liquid from each well was transferred to a 96-well plate. Finally, the plate was read in an automated microplate spectrophotometer at 570 nm as

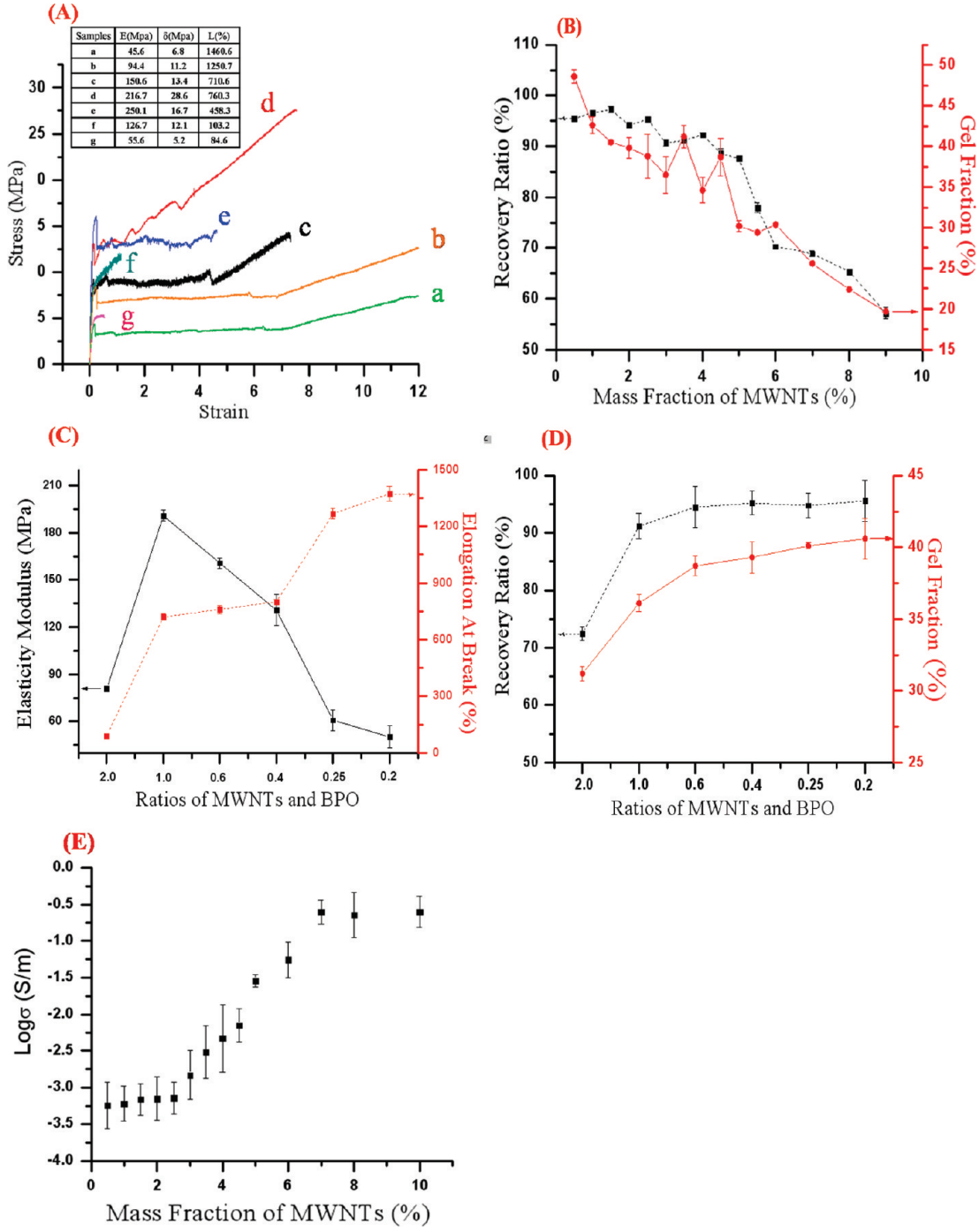

FIGURE 1. Stress−strain curves and inserted table summarized the (A) mechanical properties of the MWNTs/cPCL nanocomposites with MWNTs content of (a) 0.5, (b) 1.0, (c) 2.0, (d) 3.0, (e) 4.0, (f) 5.0, and (g) 7.0. (B) Recovery ratio and gel fraction versus mass fraction of MWNTs; the elasticity modulus and elongation at break (C) and Recovery ratio and gel fraction (D) with different ratios of BPO and MWNTs and the conductivity of the composites versus mass fraction of MWNTs (E).

reference. Every 48 h, the same test was performed as mentioned above until 168 h.

RESULTS AND DISCUSSIONS

Optimization of the Fabrication of Nanocomposites. Currently, how to obtain a composite with expected properties is an important issue. In this study, a series of parameters including the mass fraction of MWNTs and ratio of MWNTs/BPO were first studied to determine the optimized conditions of the composites fabrication. The strain−stress curves and correlative mechanical properties of the composites with different weight ratios of cPCL/AO-M were shown in Figure 1A and inserted Table, respectively (The BPO content was settled at 3 wt %). From the image, we can definitely find two crucial phenomenon: the elasticity modulus E and the tensile strength δ_b undergo a gradual increase when the MWNTs content ranges from 0 to 5 wt %, followed by an immediately decline from 5 to 10 wt %. Simultaneously, a rapid monotonic decrease

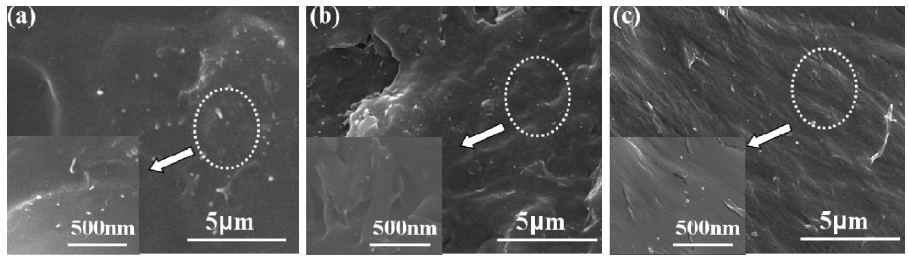

FIGURE 2. SEM images of the (a) cPCL/Raw-M, (b) cPCL/AO-M, and (c) cPCL/PEG-M with 5 wt % MWNTs and 3 wt % BPO.

in the elongation at break is observed with the increasing content of MWNTs. These results may be attributed to three factors including crystallization of cPCL, cross-linked degree and the properties of additional MWNTs. In general, as previous reports the crystallization of polymer matrix played a positive role on improving the E and δ_b of composites (44). In our system, the additional MWNTs and the cross-linking points engendered in the cross-linking reaction can extremely enhance the cPCL's crystallization because of their role as crystallization nuclei. Furthermore, the additional MWNTs can exhibit a nanoreinforcing effect because of their specific surface area (45, 46). Therefore, the improvement of the nanocomposites could be observed. However, there are also some negative effects when the MWNT content got to a high level. A reasonable explanation may be located on two aspects: on the one hand, the MWNTs are typically rigid fillers that can largely restrict the cPCL molecular chains' movement; on the other hand, higher mass fraction of MWNTs leads to more unfavorable distribution, which will extremely do harm to the mechanical properties of the composites based on previous reports (47−49). Therefore, considered these elements mentioned above, we could draw a conclusion that the optimized mass fraction of MWNTs is 5 wt %.

To evaluate the shape memory properties of these samples we focused on their changes of shape recovery ratio (Rr) and gel fraction of polymer matrix. Gel fraction is an important factor, which has close contact to the composite's cross-linked structure. In other words, it is related to the shape memory properties of those cross-linked polymers (13, 50). Panels A and B in Figure 1 show gel fraction and the shape memory recovery ratio of the samples, respectively. From this image, we can find that with the increasing of MWNTs content, Rr presented an obvious decrease from 95.6 to 57.8%. Moreover, from the gel-fraction curve, a clear decline was also observed. The results indicated that the cross-linking degree of the cPCL fell off when the mass fraction of MWNTs reached a higher level even though the initiator BPO maintained the same level. Therefore, this result suggested that some amount of BPO should also have been depleted during the cross-linking reaction. In view of strong oxidizing ability of BPO and weak reducibility of MWNTs, we could speculate that the MWNTs may be oxidized by BPO. Similarly, Fan and his co-workers reported that there would be an additional reaction of alkenes between BPO and MWNTs when the temperature was above 120 °C (51). Therefore, if we want to get an optimized composite, the weight ratio of MWNTs and BPO should be evaluated at first.

Panels C and D in Figure 1 show the mechanical properties and shape memory properties of composites with variable weight ratios of MWNTs and BPO, respectively. Herein, to carry on a convenient investigation, the content of MWNTs was settled at 5 wt % according to the result from Figure 1A, whereas the content of BPO was changed. After a comprehensive comparison, MWNTs/BPO ratio of 0.6 could be achieved in view of its best combination property.

Because we expect to prepare the electroactive SMPs, it is very necessary to study the composites' electrical conductivity. Figure 1E shows the electrical conductivity (σ) of composites with different mass fraction of MWNTs. From this image,a slight increase was observed with MWNTs original content from 0 to 3 wt % followed by a rapid rising with the weight content from 3 to 7 wt %, and the curve became steady when the content exceeded 7 wt %. It demonstrated that this kind of composites really had electrical conductivity and the percolation threshold was nearly at the weight ratio of 3 wt %.

Herein, a simple model can be utilized to explain why the conductivity exists. First, we can take the MWNTs as conductive microdomains. Later, in view of the strong aggregations effect of the MWNTs, these microdomains were further connected to form a conductive network embedded in the cPCL matrix. When the content of MWNTs exceeded the percolation threshold, more and more microdomains were brought out and the network became interconnected. Finally, an external circuit throughout the composites could be observed. Therefore, the conductivity of the composites depends on a series of factors including the conductivity of MWNTs, the contact between the MWNTs microdomains and the size of the conductive network. A similar model was also reported by Shi and his co-workers to describe the conductivity of polypyrrole (PPy) and polylactide (PLA) nanocomposites (52).

Investigation on the Properties of the Nanocomposites. Figure 2 shows SEM images of the cross sections morphology of cPCL/Raw-M, cPCL/AO-M and cPCL/PEG-M. It was evident that nearly all the MWNTs tightly embedded in the cPCL matrix and a majority of MWNTs were uniformly distributed in the cPCL matrix with the aid of SLS. This phenomenon suggests that there should be a strong interfacial effect between cPCL and MWNTs. This effect can be helpful for the composites' shape memory and electric conductivity properties. However, through further comparison, we could find that the PEG grafted MWNTs displayed much better distribution. The reasonable explana-

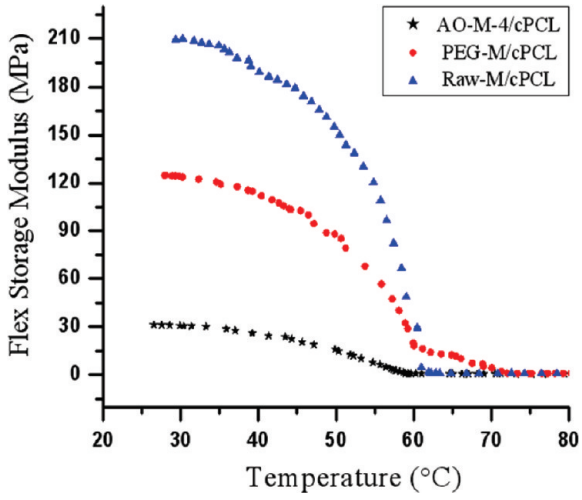

FIGURE 3. DMA curves of flex storage modulus of cPCL/Raw-M, cPCL/AO-M, and cPCL/PEG-M with 5 wt % MWNTs and 3 wt % BPO versus temperature.

tion can be attributed to the increasing hydrophilic property and closer contact between MWNTs and the polymer matrix in view of the help of PEG (53).

Figure 3 shows the change in storage modulus (E') among cPCL/Raw-M, cPCL/AO-M, and cPCL/PEG-M from DMA behaviors. All three specimens have a transition temperature range where E' suddenly decreases with the increasing temperature of about 35 °C and the dramatic change in E' can be employed to define the melting temperature (T_m) area of cPCL according to previous literatures (5, 13). On the other hand, from the cPCL/Raw-M sample curve we can observe that it first experienced a plateau (>200 MPa) below 30 °C, then a fall up to 3 orders of magnitude in the temperature range of 30−65 °C, and the E came to a low modulus plane of about 0.09 MPa. As previous reports, the tremendous change of E' usually means a large transition temperature state resulted in a great shape memory effect (54). The other specimens have similar behaviors with the cPCL/Raw-M, which also led to the shape memory properties. However, the disparity in E' values within the melting temperature range became smaller after the surface-modification of MWNTs. Smaller E' values range was mainly related to a decrease in elasticity for the specimens, which may bring a decreasing gel fraction (13). Therefore, we can infer that the surface-modification process brought some negative impacts on the mechanical and shape memory properties of the composites.

The static tensile tests and shape memory effect evaluation were carried out to confirm our results from the DMA test. As shown in panels A and B in Figure 4, both of the mechanical properties and shape memory effect of all the samples present a similar result with the DMA images. The reason is mainly attributed to the fact that acid-oxidation process can easily damage the MWNTs' structure and produce a number of defects due to the strong oxidation ability of HNO_3 (55). The defects will obviously influence the mechanical performance of the MWNTs. Moreover, more favorable performance in mechanical properties and shape memory effects were observed from the cPCL/PEG-M nanocomposite than the cPCL/AO-M sample. The reason can be summarized from two aspects: on the one hand when PEG was grafted on the surface of MWNTs through esterification method, the reactive sites may locate at defects of MWNTs in view of their higher reaction energy (56). Therefore, PEG may ameliorate or even 'repair' some defects, which caused an improvement in the mechanical and shape memory properties of the composites as shown in panels A and B in Figure 4. On the other hand, the ether bonds in PEG molecular chains could lead the composite to stronger interfacial effect and lower degree of phase separation between PEG and cPCL matrix, which could largely enhance the mechanical and shape memory property (57−60). Therefore, the introducing of the covalent PEGylation MWNTs into cPCL matrix is a more favorable choice.

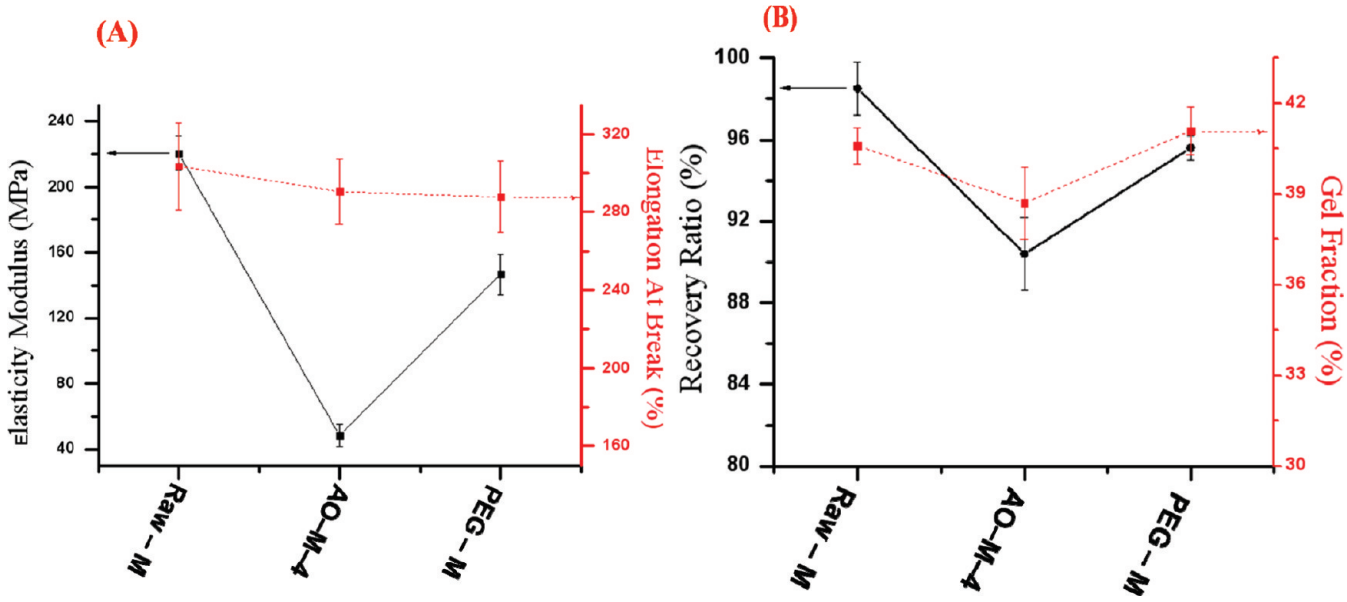

FIGURE 4. (A) Mechanical performance and (B) recovery ratio and gel fraction of cPCL/Raw-M, cPCL/AO-M, and cPCL/PEG-M with 5 wt % MWNTs and 3 wt % BPO.

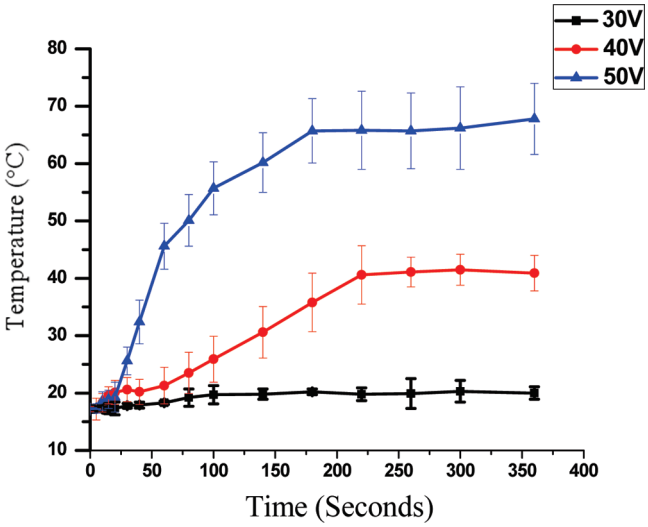

FIGURE 5. Temperature changes of the composites used as a function of decayed time when a constant voltage was applied to the samples.

Evaluation of Shape Memory Effect. Figure 5 shows the surface temperature change of the cPCL/PEG-M nanocomposite with MWNTs of 5 wt % under three constant voltages: 30, 40 and 50 V, respectively. From this image we could observe that when a 50 V voltage was applied, the sample was soon heated above 55 °C within 100 s and finally kept a steady state at nearly 70 °C. This temperature is well-above the shape recovery temperature of cPCL (nearly 55 °C). However, this phenomenon was difficult to be observed when the applied voltage was lower than 40 V. This result strongly proves that our composite enables to conduct the electrical current through the additional MWNTs and its electrical conductivity can also be utilized to stimulate the shape of composite deformed and recovered.

Figure 6 gives the photos of the shape-recovery process both in hot water at 55 °C and in 50 V applied voltage in order to obtain an intuitive comparison. It can be observed that both hot water and voltage stimuli can successfully induce shape recovery of the folded samples. However, the speed of shape recovery induced by direct thermal stimulus is much faster than that induced by electric field. This demonstrated that our composite had better reactivity in hot water than in an electric field. The less recovery time might be explained by slow heat loss and faster thermal transfer. Therefore, if we want to obtain better recovery performance in the electric field, we should achieve a higher electrical conductivity of the composite and a heat shield might be also necessary for samples in order to prevent the heat loss.

Influence of In vitro Biodegradation on Properties of the Nanocomposites. In recent years, many researchers pay much attention to the shape memory properties of SMPs before they are used in medicine. However, they always ignore a key point that some biological and physical properties of SMPs must be changed gradually due to the aging or degradation of polymers after they were applied in vivo or in vitro. So, the in vitro biodegradation evaluation is essential. Figure 7 gives changes of shape memory recovery ratio (in 55 °C hot water and 50 V supplied voltage), electrical conductivity, gel fraction, molecular weight, and mechanical properties of cPCL/Raw-M, cPCL/AO-M, and cPCL/PEG-M during 16 weeks' degradation, respectively. From the images we could observe that the cPCL/Raw-M and cPCL/PEG-M samples show more favorable biodegradability than the cPCL/AO-M. In addition, from Figure 7A, an obvious decline in shape memory recovery ratio was observed with the increasing of degradation time. It implies that the degradation process will bring a negative influence to the shape memory property. Figure 7B shows the same trend when the shape recovery is stimulated by supplied electric field. However, some evident differences, especially the decrease rate, should be noted. For example, the recovery ratio of cPCL/Raw-M samples only fell nearly 22 % after 4 weeks' degradation when we used the hot water to stimulate the recovery, but nearly 90 % decline could be observed when we took the electro-active method. There is one reasonable explanation that the electrical conductivity of these samples fell sharply during the biodegradation process. The results of electrical conductivity evaluation also proved our speculation (Figure 7B). Figure 7E displays a visual comparison of the cPCL/PEG-M composite's shape recovery effect after 4 weeks' degradation under an applied 50 V voltage. From these images we can intuitively find that the shape memory effect underwent a rapid decrease after the biodegradation process. The reason can be illustrated as follows. The SMPs exhibited shape memory properties depending on the interactions between two phases: the

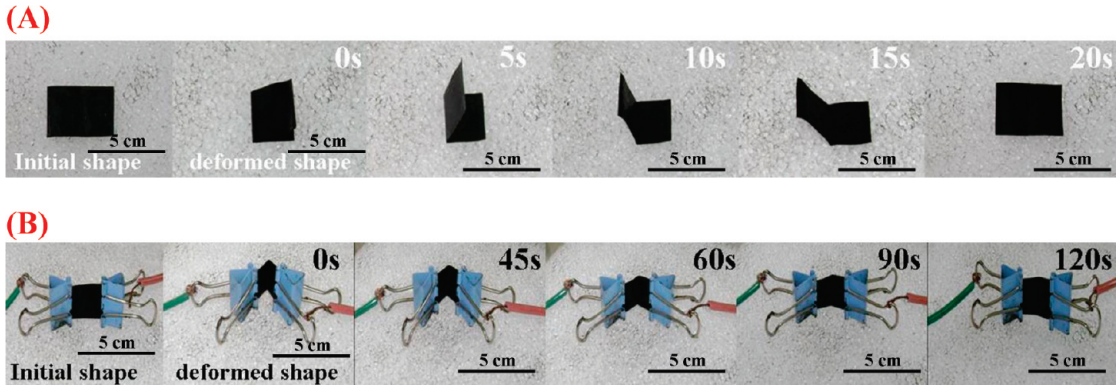

FIGURE 6. Series of digital photograph showing shape memory recovery process of the cPCL/PEG-M samples with 5 × 3 cm (length × width) (A) in the hot water at 55 °C and (B) in the supplied voltage 60 V.

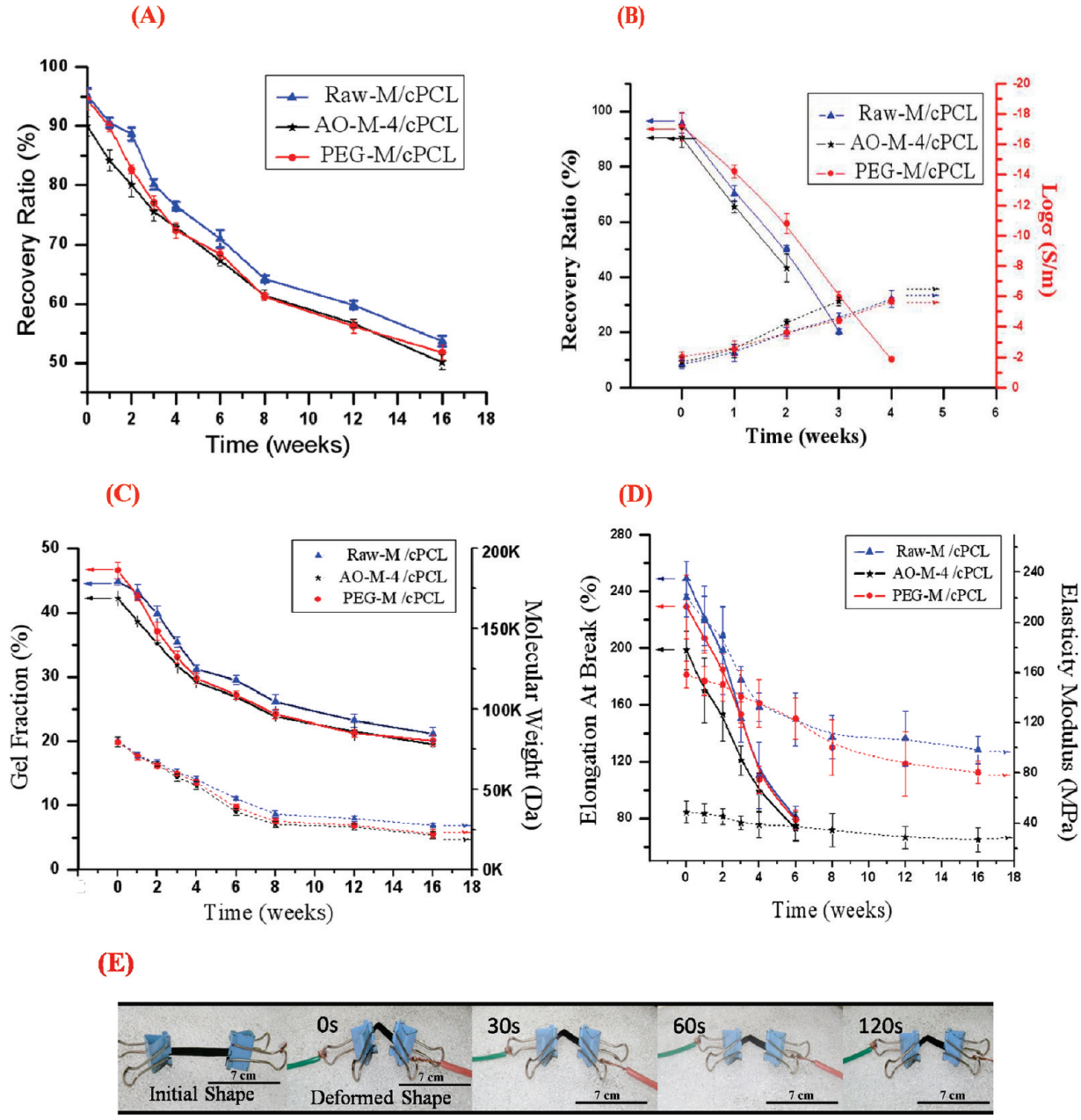

FIGURE 7. Shape memory recovery ratio (A) in the hot water at 55 °C and (B) in the supplied voltage 50 V; (C) gel fraction and molecular weight and (D) mechanical performance of cPCL/Raw-M, and cPCL/PEG-M composites versus in vitro degradation time, and (E) photographs showing the process of shape memory recovery of cPCL/PEG-M samples with 8 × 1.5 cm (length × width) after 4 weeks' degradation.

reversible phases which could memory the polymers' temporary shape and the fixable phases which could memory the polymers' initial shape. In connection with the composites, a perfect chemical network engendered from the cross-linked process is considered as the shape memory fixable phase according to the previous report (5, 13). This kind of network includes plenty of cross-linked chains and points, a great many ester-bonds are also kept in it. Therefore, during the degradation process the PBS medium entered into the inner of composites, which brought great damage to the cPCL molecular chains. More and more ester bonds would be gradually cleaved. In other words, the biodegradation process will do harm to the fixable phases. Therefore, it will cause a decrease of shape memory effect. Moreover, the disruption of cPCL's structure will largely reduce the interactions between polymer matrix and fillers, easily make the MWNTs divorce from the cPCL molecular chains, and further cause a decline in electrical conductivity.

Panels C and D in Figure 7 show the changes of gel fraction, molecular weight, and mechanical properties during the degradation process, respectively. Similarly, these results displayed a descending trend, and the reason was the same as mentioned above. The fact that the shape memory effect of biodegradable polymers decreased with the degradation time is very important, which gives us some signals on how to reserve them or how to use them as temporary implant materials.

Cytotoxicity Analysis. The cytotoxicity of cPCL/Raw-M, cPCL/AO-M and cPCL/PEG-M composites was assessed

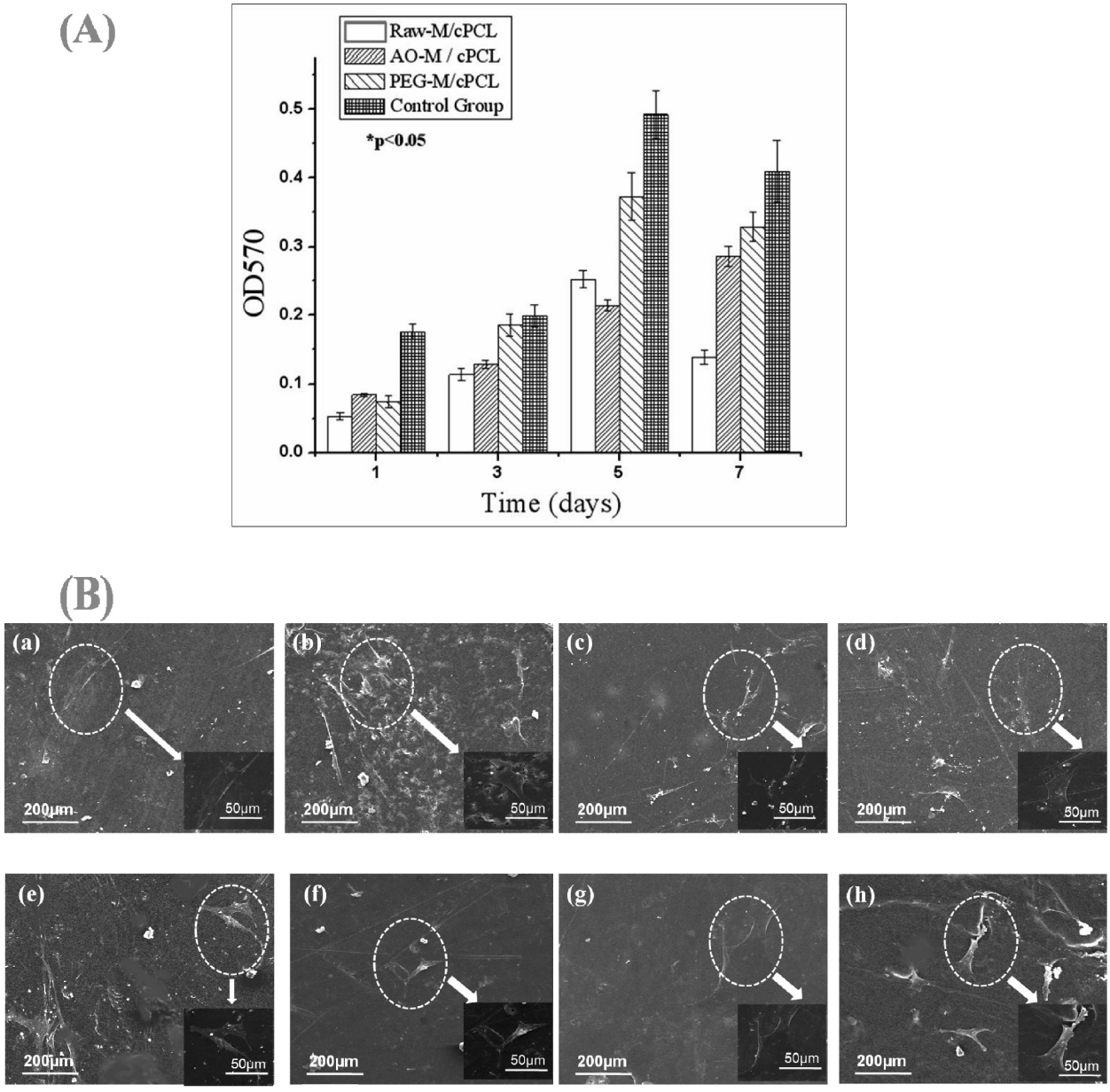

FIGURE 8. (A) MTT results of the cPCL/Raw-M, cPCL/AO-M, and cPCL/PEG-M with 5 wt % MWNTs and control group; (B) SEM image of the (a, e) cPCL/Raw-M, (b, f) cPCL/AO-M, (c, g) cPCL/PEG-M, and (d, h) control group at day 1 and day 5, respectively.

by MTT assay as shown in Figure 8A. We could find that all samples exhibited a certain extent cytotoxicity to restrain the cell viability in the first day's incubation. In addition, through further comparison cPCL/PEG-M sample exhibited higher cell viability, indicating its better biocompatibility. The following results also presented the same trend. The reason may be attributed to two aspects: first, the PEGylated sample possessed better dispersion (as shown in Figure 2C), which prevented the presence of sectional toxicity; second, the favorable biocompatibility of PEG could be a positive factor. Moreover, it should be noted that the OD values at day 7 are lower than that at day 5 because of the lack of air, space, and nutrition supplies for the cells.

Figure 8B displays the cytotoxicity of the composites evaluated by SEM. The images strongly proved those results obtained from the MTT assay. From these images, we can see that in the first day incubation, the number of the cells on the materials was far less than the control group and the morphology of the cells was also unfavorable. Through further comparison with the cPCL/Raw-M and cPCL/PEG-M samples, we could observe that the cells growing on the latter materials exhibited a better situation, and these cells displayed significantly fusiform shape and began to stretch in all directions. After 5 days' cultivation, the amount of the cells became much larger than before and the shape was completely spread out. Therefore, we could draw a conclusion that cPCL/PEG-M sample holds the better biocompatibility, which may be suitable for the biomedical application.

CONCLUSIONS

In this study, we first optimized the fabrication parameters of cPCL/MWNTs nanocomposites, mainly including the mass fraction of MWNTs and the ratio of MWNTs and BPO. A suitable parameter was achieved: the content of

MWNTs is 5 wt % and the ratio between MWNTs and BPO is 0.6. Later, the properties of all the samples including mechanical behaviors, electrical conductivity and shape memory effect were investigated and compared. The influence of the in vitro degradation of polymer matrix on its shape memory effect and mechanical properties was also studied. The changes in shape recovery and mechanical performance during the degradation process revealed a decreasing tendency for all the specimen. Finally, the biological evaluation to the composites was carried out. Two conclusions can be drawn: (1) all the samples exhibited excellent shape memory properties under the direct thermal and electrical stimulations; (2) the cPCL/PEG-M sample possessed more favorable combination properties. Therefore, the nanocomposite may be promising prospect for biomedical application.

Acknowledgment. This work was partially supported by National Natural Science Foundation of China (50773065), Programs for New Century Excellent Talents in university, Ministry of Education of China (NCET-07-0719), and Sichuan Prominent Young Talent Program (08ZQ026-040).

REFERENCES AND NOTES

(1) Lendlein, A.; Kelch, S. *Angew Chem., Int.Ed.* **2002**, *41*, 2034.
(2) Langer, R.; Tirrell, D. *Nature* **2004**, *428*, 487.
(3) Lendlein, A.; Langer, R. *Science* **2002**, *296*, 1673.
(4) Feninat, F.; Laroche, G.; Fiset, M.; Mantovani, D. *Adv. Eng. Mater.* **2002**, *4*, 91.
(5) Zheng, X.; Zhou, S.; Li, X.; Weng, J. *Biomaterials* **2006**, *27*, 4288.
(6) Neffe, A.; Hanh, B.; Steuer, S.; Lendlein, A. *Adv. Mater.* **2009**, *21*, 1.
(7) Jeong, H.; Ahn, B.; Kim, B. *Polym. Int.* **2000**, *49*, 1714.
(8) Carrizales, C.; Pelfrey, S.; Dincon, R.; Eubanks, T.; Kuang, A.; McClure, M.; Bowlin, G.; Macossay, J. *Polym. Adv. Technol.* **2008**, *19*, 124.
(9) Liu, Y.; Lv, H.; Lan, X.; Leng, J.; Du, S. *Compos. Sci. Technol.* **2009**, *69*, 2064.
(10) Yakacki, C.; Satarkar, N.; Gall, K.; Likos, R.; Hilt, J. *J. Appl. Polym. Sci.* **2009**, *112*, 3166.
(11) Koerner, H.; Price, G.; Pearce, N.; Alexander, M.; Vaia, R. *Nat. Mater.* **2004**, *3*, 115.
(12) Paik, I.; Goo, N.; Yoon, K.; Jung, Y.; Cho, J. *Key Eng Mater.* **2005**, *297−300*, 1539.
(13) Yu, X.; Zhou, S.; Zheng, X.; Guo, T.; Xiao, Y.; Song, B. *Nanotechnology* **2009**, *20*, 235702.
(14) Schmidt, A. *Macromol. Rapid Commun.* **2006**, *27*, 1168.
(15) Varga, Z.; Filipcsei, G.; Zrínyi, M. *Polymer* **2006**, *47*, 227.
(16) Yang, B.; Huang, W.; Li, C.; Li, L. *Polymer* **2006**, *47*, 1348.
(17) Chen, M.; Tsai, H.; Chang, Y.; Lai, W.; Mi, F.; Liu, C. *Biomacromolecules* **2007**, *8*, 2774.
(18) Lendlein, A.; Jiang, H.; Junger, O.; Langer, R. *Nature* **2005**, *434*, 879.
(19) Behl, M.; Lendlein, A. *Mater. Today* **2007**, *10*, 20.
(20) Ma, X.; Chang, P.; Yu, J.; Lu, P. *Starch/Starke.* **2008**, *60*, 373.
(21) Zhou, H.; Lin, Y.; Yu, P.; Su, L.; Mao, L. *Electrochem. Commun.* **2009**, *11*, 965.
(22) Leng, J.; Lv, H.; Liu, Y.; Du, S. *Appl. Phys. Lett.* **2007**, *91*, 144105.
(23) Acevedo, D.; Reisberg, S.; Piro, B.; Peralata, D.; Miras, M.; Pham, M.; Barbero, C. *Electrochim. Acta* **2008**, *53*, 4001.
(24) Luo, X.; Mather, P. *Soft Matter* **2010**, *6*, 2146.
(25) Cho, J.; Kim, J.; Jung, Y.; Goo, N. *Macromol. Rapid Commun.* **2005**, *26*, 412.
(26) Shin, J.; Jeun, J.; Kang, P. *J. Nanosci. Nanotechnol.* **2010**, *10*, 6859.
(27) Wei, G.; Zhu, Y.; Zhang, R.; Chen, Y.; Liang, J. *J. Nanosci. Nanotechnol.* **2010**, *10*, 5083.
(28) Zhao, Y.; Yuan, L.; Duan, Y. *J. Nanosci. Nanotechnol.* **2010**, *10*, 5339.
(29) Lok, B.; Ng, Y.; Liang, Y.; Hu, X. *J. Nanosci. Nanotechnol.* **2010**, *10*, 4711.
(30) Kim, S.; Roh, S. *J. Nanosci. Nanotechnol.* **2010**, *10*, 3271.
(31) Pillai, S.; Ramontja, J.; Ray, S. *Adv. Sci. Lett.* **2010**, *3*, 117.
(32) Zhou, S.; Zheng, X.; Yu, X. *Chem. Mater.* **2007**, *2*, 247.
(33) Yu, X.; Zhou, S.; Zheng, X.; Xiao, Y.; Guo, T. *J. Phys Chem C.* **2009**, *113* (41), 17630.
(34) Tasis, D.; Tagmatarchis, N.; Bianco, A.; Prato, M. *Chem. Rev.* **2006**, *106*, 1105.
(35) Sun, Y.; Fu, K.; Lin, Y.; Huang, W. *Acc. Chem. Res.* **2002**, *35*, 1096.
(36) Porter, A.; Gass, M.; Muller, K.; Skepper, J.; Midgley, P.; Well, M. *Nat. Nanotechnol.* **2007**, *2*, 713.
(37) Zhu, G.; Xu, S.; Wang, J.; Zhang, L. *Radiat. Phys. Chem.* **2006**, *75*, 443.
(38) Zhu, G.; Xu, Q.; Liang, G.; Zhou, H. *J. Appl. Polym. Sci.* **2005**, *95*, 634.
(39) Zhou, S.; Deng, X.; Yang, H. *Biomaterials* **2003**, *24*, 3563.
(40) Zhang, D.; Lan, X.; Liu, Y.; Leng, J. *Proc. SPIE* **2007**, *6526*, 101.
(41) Xiao, Y.; Gong, T.; Zhou, S. *Biomaterials* **2010**, *31*, 5182.
(42) Hofle, V.; Steiglich, W.; Vorbruggtn, H. *Angew. Chem.* **1978**, *90*, 602.
(43) Ma, X.; Yu, J.; Wang, N. *Compos. Sci. Technol.* **2008**, *68*, 268.
(44) Albuerne, J.; Marquez, L.; Muller, A.; Raquez, J. M.; Degée, Ph.; Dubois, Ph.; Castelletto, V.; Hamley, I. W. *Macromolecules* **2003**, *36*, 1633.
(45) Ajayan, P. *Chem. Rev.* **1999**, *7*, 1787.
(46) Andrews, R.; Weisenberger, M. *Curr. Opin. Solid State Mater.* **2004**, *8*, 31.
(47) Zhang, D.; Kandadai, M.; Cech, J.; Roth, S.; Curran, S. *J. Phys. Chem. B* **2006**, *110*, 12910.
(48) Wang, S.; Shen, L.; Zhang, W.; Tong, Y. *Biomacromolecules* **2006**, *6*, 3067.
(49) Shen, M.; Wang, S.; Shi, X.; Chen, X.; Huang, Q.; Petersen, E.; Pinto, R.; Baker, J., Jr.; Weber, W., Jr. *J. Phys. Chem. C* **2009**, *113*, 3150.
(50) Liu, C.; Chun, S.; Mather, P. *Macromolecules* **2002**, *35*, 9868.
(51) Fan, H.; Cheng, X.; Mei, L.; Yan, S.; Wei, C.; Ming, C. *Chem. Res. Appl.* **2006**, *18*, 53.
(52) Shi, G.; Rouabhia, M.; Wang, S.; Dao, L.; Zhang, Z. *Biomaterials* **2004**, *25*, 2477.
(53) Xu, F.; Xu, J.; Ji, J.; Shen, J. *Colloids Surface. B* **2008**, *67*, 67.
(54) Byung, K.; Sang, Y.; Mao, X. *Polymer* **1996**, *37*, 5781.
(55) Datsyuk, V.; Kalyva, M.; Papagelis, K.; Parthenios, J.; Tasis, D.; Siokou, A.; Kallitsis, J.; Galiotis, C. *Carbon* **2008**, *46*, 833.
(56) Liu, Z.; Sun, X.; Ratchford, N.; Dai, H. *ACS Nano* **2007**, *1*, 50.
(57) Ajayan, M.; Tour, J. *Nature* **2007**, *447*, 1066.
(58) Fu, S.; Guo, G.; Wang, X.; Zhou, L.; Liu, T.; Dong, P.; Luo, F.; Gu, Y.; Shi, X.; Zhao, X.; Wei, Y.; Qian, Z. *J. Nanosci. Nanotechnol.* **2010**, *10*, 711.
(59) Li, X.; Kong, X.; Shi, S.; Gu, Y.; Yang, L.; Guo, G.; Luo, F.; Zhao, X.; Wei, Y.; Qian, Z. *Carbohydr. Polym.* **2010**, *79*, 429.
(60) Fu, S.; Guo, G.; Wang, X.; Zhou, L.; Liu, T.; Dong, P.; Luo, F.; Gu, Y.; Shi, X.; Zhao, X.; Wei, Y.; Qian, Z. *J. Phys. Chem. B* **2009**, *113*, 16518.

AM100692N